Fluorescence Correlation Spectroscopy of Enzymatic DNA Polymerization†

Sofie Björling, Masataka Kinjo,‡ Zeno Földes-Papp, Ebba Hagman, Per Thyberg, and Rudolf Rigler*

Department of Medical Biophysics, MBB, Karolinska Institute S-171 77, Stockholm, Sweden

Received March 26, 1998; Revised Manuscript Received June 29, 1998

ABSTRACT: We show that fluorescence correlation spectroscopy (FCS) can be used as a reliable, simple, and fast tool for detecting products of the polymerase chain reaction (PCR). By use of autocorrelation experiments, it is demonstrated that fluorescent 217-bp DNA fragments can be detected at very low initial ss M13mp18$^+$ DNA and tetramethylrhodamine-4-dUTP concentrations and that these polymers are cleaved by the chosen restriction enzymes. A FCS calibration curve is presented, where the translational diffusion times of different size DNA fragments are plotted versus the number of base pairs they contain. At zero and very low template concentrations a large "background" species emerges, which is a reflection of the experimental conditions chosen and the extremely high sensitivity of FCS. The relative amount of nonspecific product formation is less than 1%. The ease by which a FCS measurement can be performed (a few minutes at most) also enables the technique to be used as an effective screening method.

Fluorescence correlation spectroscopy (FCS)[1] is based on the temporal intensity fluctuations of molecules excited to fluorescence by a stationary light source. The fluorescent particles move through a small region (volume element) defined by the focused laser beam that is exciting them. Thermal fluctuations of the molecules are observed and correlated. The autocorrelation function obtained provides information about the mechanisms and rates of the processes generating the fluctuations. When translational diffusion of the fluorescing molecules is the only process resulting in intensity fluctuations, one can obtain information about the size of the particles studied at a fixed dimension of the volume element. The residence time of a molecule in the volume element is dependent on its diffusion constant, which in turn is dependent on the size of the particle. From the amplitude of the autocorrelation function one obtains the number of molecules within the volume element at each particular time, and thus the sample concentration. FCS has been described in detail elsewhere (*1*−*12*).

There is often a need to analyze the nature of DNA fragments. For this purpose one takes advantage of the polymerase chain reaction (PCR), where the target sequence of interest is amplified. PCR has proved to be a powerful tool for biochemists as well as molecular biologists. It is necessary to develop rapid, simple, and sensitive detection systems and techniques in order to benefit fully from the rapid target amplification. We present herein results of a fast and sensitive FCS method that detects PCR products after the incorporation of fluorescent nucleoside triphosphates into DNA. These results show that FCS provides considerably higher sensitivity than conventional detection methods.

To detect PCR products by FCS, they need to be fluorescent. In this work this is achieved by adding tetramethylrhodamine-4-dUTP to the PCR reaction mixture in addition to the other four dNTPs, such that during the amplification reaction some of the dTTPs to be incorporated will be exchanged for tetramethylrhodamine-4-dUTP. It is then possible to measure the correlation function of the PCR product using FCS, and from it the size of the PCR product can be estimated. Such a measurement can be performed in a few seconds and is thus a remarkable increase in efficiency compared to gel electrophoresis. In this study we were interested in finding some parameters for such DNA amplification. The amount of DNA template, tetramethylrhodamine-4-dUTP, and primer in the reaction mixture were varied. We investigated the nature of the products by exposing them to exonuclease and restriction enzyme digestion. In addition, we developed a calibration curve for DNA fragments of different lengths using FCS. This was achieved by graphing the translational diffusion time of the fragments studied versus the number of DNA base pairs they contain. Using this calibration curve, one can estimate the length of a DNA fragment from its diffusion time.

MATERIALS AND METHODS

Sample Preparation. Fluorescently labeled DNA, a 217-bp region of single-stranded (ss) M13mp18$^+$ (Pharmacia Biotech, Sweden), was synthesized by Taq DNA polymerase (Pharmacia Biotech, Sweden) in the presence of tetramethylrhodamine-4-dUTP (Rho-4-dUTP, FluoroRed, Amersham), using the primers 5′-d(AA AGG GGG ATG TGC TGC AAG GCG) and 5′-d(GC TTC CGG CTC GTA TGT TGT GTG) (Dynal). The polymerase reaction was carried out in a 60

† This study was supported by the Swedish Research Council for Engineering Sciences and the Swedish National Board for Industrial and Technical Development. S.B. obtained financial support from the National Board of Health and Welfare. M.K. obtained a fellowship from Japan Society for Promotion of Science and the Itho Foundation (Sapporo). Z.F.-P. received a fellowship from the foundation Wenner-Gren (Sweden).

* Corresponding author.

‡ Present address: Laboratory of Molecular Physiology, Research Institute for Electronic Science, Hokkaido University, Sapporo, Japan.

[1] Abbreviations: FCS, fluorescence correlation spectroscopy; TMR-4-dUTP, tetramethylrhodamine-4-(deoxyuridine triphosphate); PCR, polymerase chain reaction; FET, Förster energy transfer.

S0006-2960(98)00694-1 CCC: $15.00
Published on Web 08/26/1998

μL solution with 3.4−85 μM tetramethylrhodamine-4-dUTP, 166.7 μM dNTPs, 2 × 2.5 pmol of primer, 5 units of Taq DNA polymerase in the presence of 22 mM Tris-HCl (pH 8.3, 20 °C), 42 mM KCl, 1.7 mM $MgCl_2$, with and without 8×10^{-5} % (v/v) Tween 20 using a PTC-150 MiniCycler (MJ Research, Inc.). Most PCR experiments were performed adding 7×10^{-13} M ss M13mp18$^+$ template to the reaction mixture. In one set of experiments the template concentrations were varied between 0 and 7×10^{-13} M. PCR was performed in 25 cycles and the reaction mixtures were subsequently applied to a MicroSpin column (S-200 HR, Pharmacia Biotech, Sweden) in order to separate the DNA product from unincorporated tetramethylrhodamine-4-dUTP.

For the calibration curve, double-stranded DNA, 500 and 50 bp regions of λ phage (GeneAmp DNA amplifications reagent kit product insert, Perkin-Elmer Corp.), a 217-bp region of ss M13mp18$^+$, and a 343-bp region of pBluescript II SK(+) [Technical Handbook of Molecular Biology (1992) pp 14−27, Dynal AS, Norway], were synthesized by PCR. The PCR products were collected by ethanol precipitation and then served as templates for the Klenow fragment of DNA polymerase I (Boehringer Mannheim, Germany). The labeling reactions were carried out in 20 μL of solution with 50 μM tetramethylrhodamine-4-dUTP, 25 μM dTTP, 50 μM dATP, 50 μM dGTP, 50 μM dCTP, 2 μM primer, and the Klenow fragment (4 units) in the presence of 40 mM Tris-HCl (pH 7.4), 50 mM NaCl, 10 mM $MgCl_2$, and 10 mM DTT. After incubation at 37 °C overnight, the reaction mixture was applied to a Sephacryl S-400 column (1.5 × 6 cm) (Pharmacia Biotech, Sweden) with a buffer containing 10 mM Tris-HCl (pH 8.0), 1 mM EDTA, and 0.1 M NaCl, to separate the product from unincorporated tetramethylrhodamine-4-dUTP. The eluent from the column was subjected to FCS measurements without further concentration.

Sample Degradation. Degradation of the fluorescently labeled PCR products were performed with T7 exonuclease (wild-type T7 polymerase, a gift from Professor Arne Holmgren, Karolinska Institute). The conditions and the proof of complete enzymatic degradation by T7 exonuclease are published elsewhere (*13*). Deoxyribonuclease I (DNase I, Boehringer Mannheim, Germany) and the restriction enzymes *Sma*I and *Hae*III (Boehringer Mannheim, Germany) were used according to the manufacturer's recommendations.

FCS Analysis. The FCS measurements were carried out at room temperature using confocal excitation and detection as described by Rigler et al. (*7*). Data analysis was performed using an in-house developed analysis program based on the Marquardt nonlinear least-squares algorithm (*14*). The normalized intensity autocorrelation function for diffusing particles can be described as

$$G(\tau) = 1 + \frac{1}{N}\frac{1}{1+\frac{\tau}{\tau_D}}\left[\frac{1}{1+\left(\frac{\omega_0}{z_0}\right)^2\frac{\tau}{\tau_D}}\right]^{1/2} \quad (1)$$

where N is the mean number of molecules within the sample volume element, τ is the channel time, τ_D is the characteristic diffusion time, ω_0 is the radius, and z_0 is the half-length of the sample volume element. τ_D is related to the translational diffusion constant D of the fluorescing species by $\tau_D = \omega_0^2/4D$.

To investigate the number of components with different diffusion times, the FCS measurements were analyzed according to the CONTIN (*15*, *16*) algorithm:

$$G(\tau) = 1 + \frac{1}{N}\int_{\tau_D}\frac{P(\tau_D)}{1+\frac{\tau}{\tau_D}}\left[\frac{1}{1+\left(\frac{\omega_0}{z_0}\right)^2\frac{\tau}{\tau_D}}\right]^{1/2} d\tau_D \quad (2)$$

In this analysis a distribution of diffusion times, $P(\tau_D)$, is determined after introducing a regularization of the distribution function to exclude solutions that show false components in addition to the dominating real ones.

The diffusion constant D is related to the frictional coefficient, which depends on the types of bodies undergoing diffusion in a continuous medium of defined viscosity. A proper hydrodynamic model treating the deviations from rodlike conformations in an appropriate way is used in ref *18*. For DNAs in the rodlike limit we analyzed the experimental data by

$$\tau_{D,L} = \left(\frac{3\pi\eta_0\omega_0^2}{4kT}\right)L\frac{1}{\ln p + \gamma} \quad (3)$$

where k is the Boltzmann constant, T is the absolute temperature, η_0 is the viscosity of the solution, ω_0 is the half-axis (radius) of the volume element, L is the length of the rodlike DNA at given length/diameter p, and γ is an end-effect correction (*18*).

Lifetime Analysis. The instrumentation used for the fluorescence lifetime measurements has been described in detail earlier (*17*). A mode-locked, synchronously pumped dye laser (Coherent 200 Ar−ion pump and Coherent 702 dye laser with cavity dumper) was used to excite the sample at 565 nm. The fluorescence was collected at 590−620 nm with a Hamamatsu (R1564U) microchannel plate photomultiplier set up in a time-correlated single photon counting mode. The time-resolved fluorescence decays were analyzed according to a standard multiexponential decay function also utilizing the Marquardt nonlinear least-squares algorithm (*14*).

RESULTS

Diffusion of DNA Fragments. The PCR products were easily quantified by FCS. Figure 1 panel A shows the autocorrelation function of free tetramethylrhodamine-4-dUTP, and panel B depicts the same function of a PCR product obtained with 7×10^{-13} M ss M13mp18$^+$ initial template concentration. When the experimental FCS curves are modeled by eq 1 above, one can evaluate the translational diffusion times of the samples. It will depend on the volume element and thus on the magnification provided by the microscope objective used. The diffusion times obtained (75 μs for TMR-4-dUTP and 1.2 ms for the PCR product) were just as would be expected from the relative molecular weights of the samples. The reproducibility between different preparations and FCS experiments was on the order of 5%. PCR samples prepared in this manner were also detected as having a band of the correct size by gel electrophoresis. When using FCS we were able to measure the products when they were diluted by several orders of magnitude. The translational diffusion time depends on the length of the

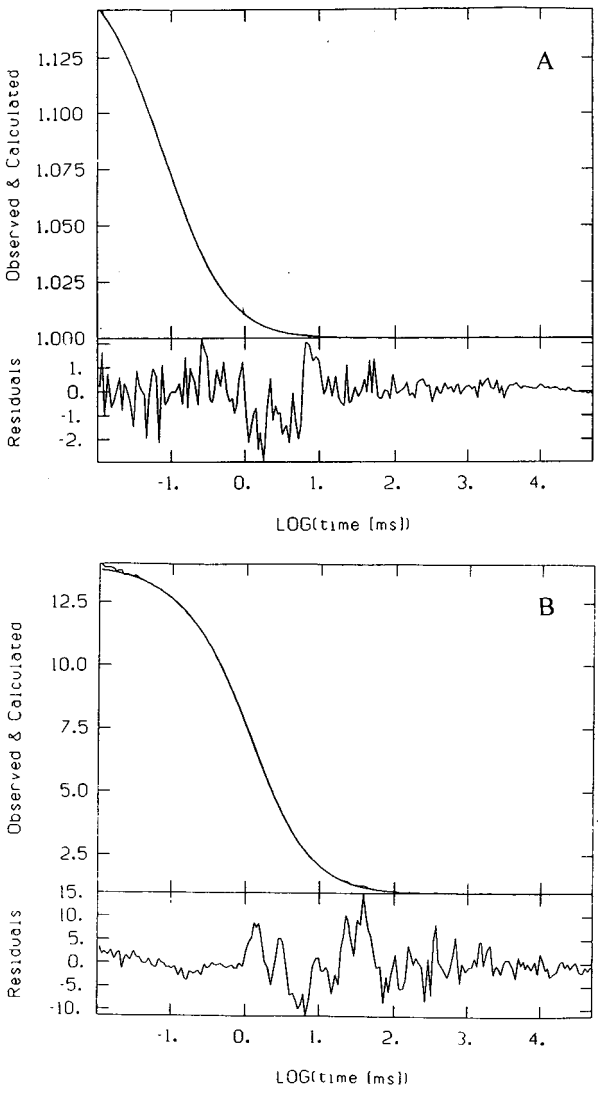

FIGURE 1: Measured and calculated autocorrelation curves. The amplitudes are related to the inverse number of fluorescence molecules (see eq 1). The objective "Plan-Neofluo 63/1.2 W korr, Zeiss, Germany" was used. (A) Free tetramethylrhodamine-4-dUTP (1 nM). The diffusion time is 75 μs. (B) ds DNA (217-bp) amplified by PCR in the presence of 30 μM tetramethylrhodamine-4-dUTP. The diffusion time is 1.2 ms. The lower parts of the panels show the difference between the measured and calculated autocorrelation functions as weighted residuals. The weighting factor is calculated according to the procedure in ref *4*.

DNA. A calibration curve for determining the molecular weight of a DNA fragment from its diffusion time was therefore developed and is presented in Figure 2A. The translational diffusion times are plotted versus the number of base pairs of the products. As a comparison to the experimental data, a curve calculated according to the study of frictional coefficients of restriction fragments of different lengths (*18*) is plotted as the solid line in Figure 2A. Figure 2B shows the time distribution of the diffusion times of the different DNA fragments investigated and is obtained by analyzing the FCS data using eq 2.

Incorporation of TMR-4-dUTP. The PCR reaction was performed at four different tetramethylrhodamine-4-dUTP concentrations, ranging from 3.4 to 85 μM. The products were subjected to exonuclease degradation. By monitoring the amplitude of the correlation function (eq 1) before and after this reaction, the number of fluorescent bases released

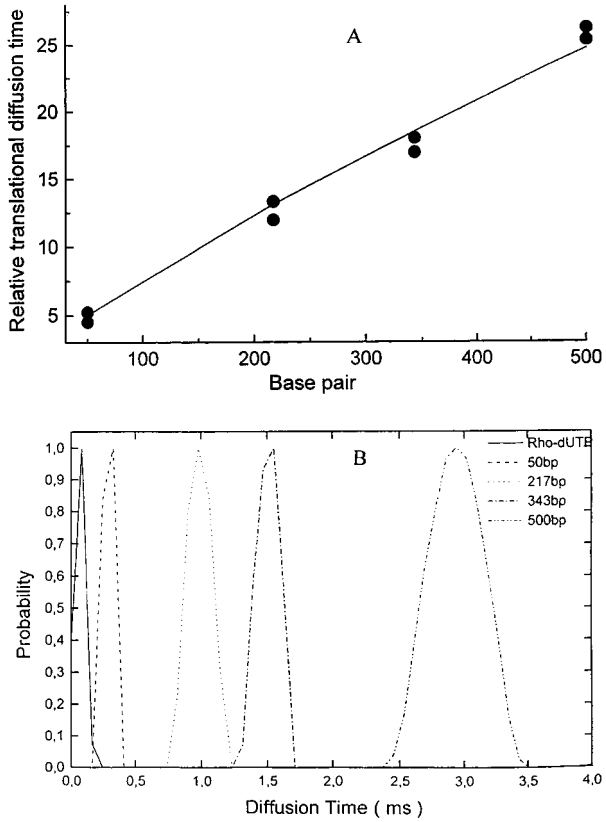

FIGURE 2: Translational diffusion times of DNA fragments of different lengths measured by FCS. The objective "Plan-Neofluo 63/1.2 W korr, Zeiss, Germany" was used. (A) Diffusion times versus the number of base pairs of the DNA. The solid line is calculated according to eq 3 for rodlike objects given in ref *18*, using here diffusion times of the DNA fragments which are normalized to that of free tetramethylrhodamine-4-dUTP. L is given by the height of a base pair (3.4 Å) times the number of base pairs. d is the diameter of the hydrated DNA [27 Å in eq 3 (see ref *18*)]. The parameter γ is set to 0.39. (B) Distribution of the translational diffusion times of different DNA fragments.

Table 1: Effect of Initial Tetramethylrhodamine-4-dUTP Concentration in the PCR on the Number of Tetramethylrhodamine-4-dUMP Molecules Released during Exonuclease Digestion of DNA[a]

TMR-4-dUTP added (μM)	molar ratio, TMR-4-dUTP/dTTP	no. of TMR-4-dUMP released per DNA	no. of TMR-4-dUTP incorporated per AT base pair
3.4	1:49	3.3	1:31.5
16.9	1:9.9	9.4	1:11.1
30.0	1:5.6	11	1:9.5
85	1:1.9	30[b]	1:3.5

[a] DNA sample was made from 7×10^{-13} M ss M13mp18$^+$, using a $\times$63 objective. [b] Incomplete degradation to give evidence of oligomeric reaction intermediates during the enzymatic reaction.

was found. The results are shown in Table 1. For the experiment performed at 85 μM tetramethylrhodamine-4-dUTP, we used experimental conditions in which the degradation of the DNA is incomplete, e.g., exonuclease concentrations much lower than 200 nM and no preincubation step to provide full 3′ → 5′ exonuclease activity (see ref *13*). It was therefore possible to obtain evidence of oligomeric reaction intermediates in the time window of the measurement. It is evident from the data of Table 1 that even at a very low tetramethylrhodamine-4-dUTP concentration a significant amount of fluorescent bases were released and therefore have been incorporated. It was thus decided

to use low dye concentrations since it proved to be sufficient to produce detectable PCR products.

Lifetime Analysis of TMR-Labeled DNA Fragments. Time-resolved fluorescence measurements on free tetramethylrhodamine-4-dUTP and the fluorescent PCR product were performed in order to elucidate the quantum yield difference of the incorporated and free dye. The quantum yield is generally proportional to the lifetime of the fluorophore. In estimating the difference in quantum yield it is assumed that the absorbance of free tetramethylrhodamine is the same as for the bound dye. Figure 3 shows the fluorescence time decays obtained in these experiments. The data were analyzed with a (multi)exponential model and the results are shown in Table 2. The free tetramethylrhodamine-4-dUTP exhibits a simple one-exponential time decay (Figure 3A), while the PCR product shows a more complicated time dependence, best described with three exponentials (Figure 3B). By calculation of the average lifetime of the PCR product ($\tau_{av} = 0.72$ ns), it becomes clear that the quantum yield of tetramethylrhodamine-4-dUTP decreases to less than a third of its free value when incorporated into the DNA.

Background Formation by PCR. PCR reactions were performed at decreasing ss M13mp18$^+$ concentrations in order to investigate the effect of initial template concentration on the product formation. The samples were subsequently investigated by FCS and the diffusion times obtained after analyzing the data using eq 1 are shown in Table 3. The final concentrations of amplified products in the PCR mixes are given as well and are obtained from the number of molecules measured within the volume element (N in eq 1). The time distribution of the diffusion times, obtained from eq 2, are shown in Figure 4. Panels A, B, and C of Figure 4 show the time distribution obtained at 7×10^{-13} M, 7×10^{-17} M, and 0 M initial ss M13mp18$^+$ concentration, respectively. A long diffusion time component was observed when the template was omitted or was present at low concentrations, as can be seen in Figure 4B,C and Table 3. The lower the initial ss M13mp18$^+$ concentration, the smaller the amount of the 1.7 ms product (the 217-bp product) and the more of a longer component is obtained. It appears as if this "background" product is heterogeneous between the different samples, since the long diffusion times differ between them. These samples were also put on agarose gels in order to discern their electrophoretic size. A single band of the correct size was found for the samples obtained at the highest initial template concentrations, but due to the low concentrations of the samples containing the background, no bands could be found when they were applied to agarose gels. The "background" was observed by FCS even after all the reagents had been exchanged to ensure that it was not a contaminant DNA template. Without the addition of template, less than 1% formation of nonspecific products was found in comparison to the amplification performed at 0.7 pM template. To investigate if the background is a product of the primers, the PCR reaction was performed without DNA template but with two different primer concentrations. The results obtained show that half as much "background" product was formed when the primer concentration was decreased to half (data not shown) and indicate that the background is some sort of a primer product.

Nuclease Degradation of DNA Fragments. The "background" was subjected to DNase digestion. A decrease in diffusion time from 3 ms to 260 μs upon this nonspecific degradation to oligonucleotides was found (data not shown). The products of the specific and nonspecific PCR reactions were subjected to a couple of restriction enzymes chosen to detect and cleave the 217-bp PCR product at a specific sequence site. Detecting the change in the number of molecules in the volume element during restriction enzyme digestion has been shown to be an efficient way of monitoring the reaction (*19*). *Sma*I will produce 95- and 122-bp fragments and *Hae*III will produce 141- and 76-bp fragments

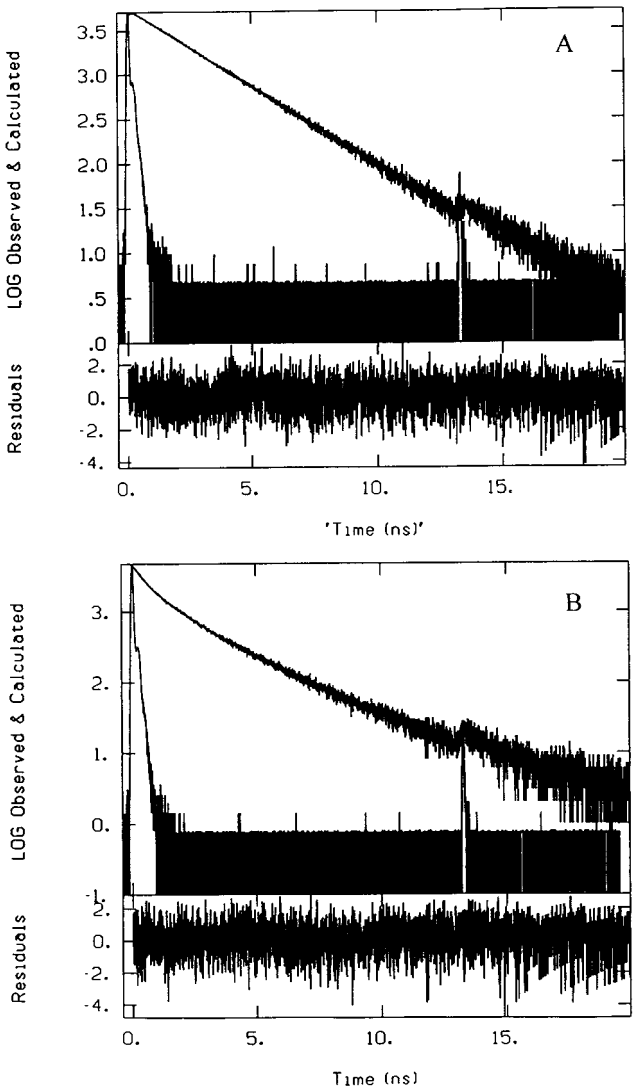

FIGURE 3: Measured and calculated fluorescence decay curves. The ordinate depicts the logarithm of the fluorescence intensity, and the abscissa the time in nanoseconds. The decaying fluorescence signal is given by the fluorescence collected with the emission polarizer set at the magic angle (54.7°) relative to the laser polarization. It is free from polarization and rotation effects and contains information about the fluorescence lifetimes modeled by a multiexponential decay function. The curve corresponding to the excitation pulse is clearly distinguished by the time scale. The random spikes are caused by photon shot noise. The calculated fluorescence decay curve is obtained by convolution of the modeled true fluorescence decay with the instrument response (laser pulse). The calculated values were fitted to the measured curve by a least-squares fitting procedure (*14*). The weighted differences between the measured fluorescence decay and the calculated values are given in the residual plots (lower parts). (A) Free tetramethylrhodamine-4-dUTP (100 nM). (B) ds DNA (217-bp) amplified by PCR in the presence of 85 μM tetramethylrhodamine-4-dUTP.

Table 2: Normalized Amplitudes and Lifetimes Obtained after Analysis of Time-Resolved Fluorescence Measurements of Tetramethylrhodamine-4-dUTP and 217-bp ds DNA[a]

	a_1	τ_1 (ns)	a_2	τ_2 (ns)	a_3	τ_3(ns)	τ_{av}[b] (ns)
TMR-4-dUTP	1	2.4 ± 0.0029[c]					
217-bp ds DNA	0.046	3.5 ± 0.39	0.45	0.99 ± 0.057	0.51	0.23 ± 0.016	0.72

[a] DNA sample was made from 7×10^{-13} M ss M13mp18$^+$ and 85 μM tetramethylrhodamine-4-dUTP. [b] Calculated weighted averaged lifetime. [c] Standard deviation of individual fits.

Table 3: Effect of Initial Template Concentration on Diffusion Times, Final Concentrations of All Amplified Products in the PCR Mixes, the Amplification Factor of the Desired 217-bp Product As Measured by FCS[a]

initial ss M13mp18$^+$				
concn (M)	no. of molecules	diffusion times (ms) [fractions][b]	total final concn (nM)	amplification factor for 1.7 ms product
7×10^{-13}	2.5×10^7	1.7 [1.0]	28	4×10^4
7×10^{-15}	2.5×10^5	1.7 [1.0]	24	3×10^6
7×10^{-17}	2.5×10^3	1.7 [0.7] 4.7 [0.3]	1.6	2×10^7
7×10^{-18}	250	1.7 [0.6] 5.5 [0.4]	0.52	4×10^7
7×10^{-19}	25	1.7 [0.2] 3.4 [0.8]	0.26	7×10^7
0	0	3.0	0.22	

[a] DNA sample was made from 3.4 μM tetramethylrhodamine-4-dUTP, using a ×40 objective. Standard deviations of individual fits are less than 2%. [b] Values in brackets indicate the relative amount of the components.

upon digesting the 217-bp DNA molecule. This would result in twice as many molecules in the FCS volume element and a decrease in the diffusion time upon complete cleavage. As can be seen in Table 4, the number of molecules increased by a factor of 2 and the diffusion time decreased upon cleavage of the 217-bp product by *Hae*III and *Sma*I, just as was expected. (The difference in diffusion times of the 217-bp PCR product between Tables 3 and 4 is due to the different magnifying objectives used for the FCS measurements.) The background was also cleaved by these enzymes, as found by decreasing diffusion times and increasing number of molecules in the volume element (data not shown).

DISCUSSION

Incorporation of TMR-4-dUTP. Here we describe a FCS-based PCR assay in which fluorescently labeled nucleoside triphosphates are included. During PCR the fluorescent nucleotides are incorporated into DNA by the 5′ → 3′ polymerase activity of Taq DNA polymerase. Amplification is detected by measuring the fluorescence autocorrelation function after the PCR is completed. We use parameters for PCR product analysis such as diffusion time, number of molecules, and their relative fractions. PCR allows the amplification of specific nucleic acids (DNA and RNA) with defined nucleotide lengths and sequences in a complex mixture of other nucleic acids and substances. It is being used extensively in any situation that requires known target flanking regions to which short oligonucleotide primers can specifically bind. Theoretically, PCR is capable of amplifying one single copy of target DNA sequence. In practice, depending on the species and the method for amplification, about 10−100 copy numbers are presently the limit when DNA-derived fluorescent primers are used (*20*). The study presented herein shows that several experimental advantages can be gained by using fluorescent nucleotides for labeling DNA. The PCR conditions used here were under investigation for discriminating between specific and nonspecific

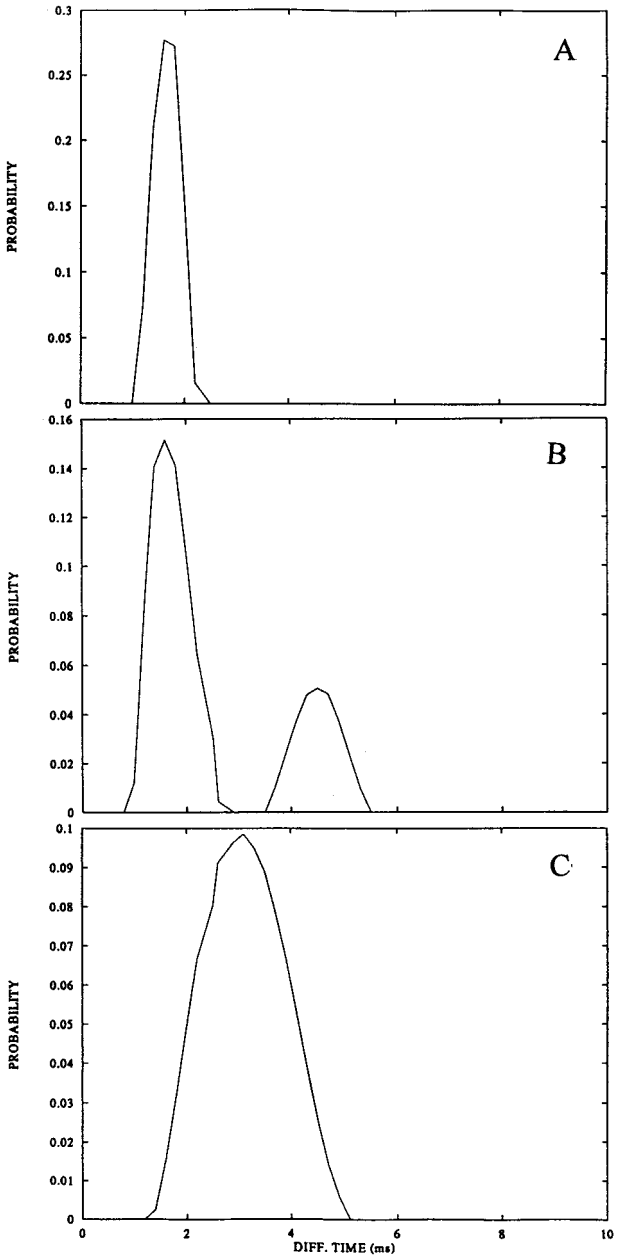

FIGURE 4: Distribution of the translational diffusion times of PCR samples obtained at different initial template concentrations, as measured by FCS. The objective "Plan-Neofluo 40/0.9 Imm. Korr., Zeiss, Germany" was used. (A) Initial ss M13mp18$^+$ concentration 7×10^{-13} M. (B) Initial ss M13mp18$^+$ concentration 7×10^{-17} M. (C) Initial ss M13mp18$^+$ concentration 0 M.

amplification by means of FCS autocorrelation analysis. An approximately linear relationship between the incorporated number of tetramethylrhodamine-4-dUTP molecules and the molar ratio of tetramethylrhodamine-4-dUTP/dTTP in the PCR was found (Table 1). A similar relationship was found when the count rate per molecule was monitored by

Table 4: Effect on Diffusion Times and Total Number of Molecules in the Volume Element upon Endonuclease Digestion of 217-bp ds DNA[a]

	217-bp ds DNA	DNA after *Hae*III	DNA after *Sma*I
τ_D (ms)	1.2	0.93	0.94
no. of molecules	1	1.83 ± 0.23[b]	2.06 ± 0.47

[a] DNA sample made from 7×10^{-13} M ss M13mp18$^+$ and 3.4 μM tetramethylrhodamine-4-dUTP, using a $\times$63 objective. Number of molecules in the volume element is normalized to the value obtained before the start of the digestion. [b] Standard deviation between different experiments.

performing FCS measurements on PCR products containing fluorescein-dUTP (*21*). With Cy3-dUTP and Cy5-dUTP as labels, labeling conditions were reported for PCR yielding probes with 20 dyes/kilobase (*22*). We have developed a cassette technique for template-directed synthesis of short DNA fragments in primer extension reactions with fluorescent dNTPs in order to determine experimentally the probability density of stop and pause sites during the enzymatic polymerization process (*23*). We provided an experimental method for estimating the nucleotide length of the target and for quantifying byproducts by comparison with the relative migration distance of cassettes in chemiluminescence images taken from the blotted gel. A modified application of this method was a template system consisting of consecutive nucleotides of the same base, for example 18 As in a row. By use of tetramethylrhodamine-6-dUTP instead of nonlabeled dTTP, it was found by Földes-Papp et al. (*23*) that the fluorescent dUTP is able to substitute entirely for the normal nucleotide at a short target length N of the template ($N = 41$). However, the ability to incorporate tetramethylrhodamine-6-dUTP opposite to A in the template DNA varied significantly among the polymerases studied [Klenow enzyme, Taq DNA polymerase, Pwo DNA polymerase, Vent DNA polymerase, AMV and HIV reverse transcriptases, and DNA polymerase X from Boehringer Mannheim (Roche Molecular Biochemicals, Germany)]. Furthermore, tetramethylrhodamine-6-dUTP might have some inhibitory effect on the $3' \rightarrow 5'$ exonuclease activity of Vent polymerase. FCS is well-suited to assaying the progress of polymerization reactions when fluorescent nucleotides are incorporated into the reaction (amplification) products or/and amplification primers 5′-labeled with fluorescent reporter dyes are used. It has been reported that complete labeling can be obtained with a tailor-made polymerase (*24*).

Diffusion of DNA Fragments. Several experimental and theoretical analyses of the translational properties of rodlike molecules have been published (*18*, *25*−*28*). We have found that the experimental results shown in Figure 2A agree well with the equation for rodlike conformations (*18*), and a curve calculated according to this equation is plotted as the solid line in the figure. This shows that the translational diffusion time of ds DNA is best simulated by a rodlike model. It is clear that an almost linear relationship between the length and the translational diffusion time of the DNA exists and that from the diffusion time of a DNA fragment one can estimate its length. This relationship holds true up to at least 500 base pairs.

Quenching and Förster Energy Transfer. Fluorescence is very sensitive to changes in the environment of the fluorophore. One way to probe this environment is to investigate the decay of the fluorescence as a function of time. This is the basis for the time-resolved fluorescence data reported herein, where the fluorescence decay is analyzed in terms of lifetimes. As can be seen in Figure 3, the decay curve of the fluorophore (tetramethylrhodamine-4-dUTP) is largely affected by its incorporation into the DNA. From exhibiting a simple one-exponential decay (Figure 3A) with a lifetime of 2.4 ns, its decay becomes much more complicated, displaying three different lifetimes, upon its incorporation into the DNA (Figure 3B). The observation of three lifetimes is an indication that there are three different populations of the fluorophore in the DNA, each one with a different environment affecting its emission decay, assuming that the absorbance of the tetramethylrhodamine in its bound and nonbound states is the same. The lifetimes and amplitudes of the fluorescence are given in Table 2. A weighted average of the lifetime of the DNA has been calculated (0.72 ns), and from that one can see that the lifetime of the fluorophore is decreased to less than a third of its free value (2.4 ns) upon incorporation into the DNA. This indicates that the fluorophore is somehow quenched by its surroundings. It is known that rhodamine can be quenched by electron transfer to G (*29*−*32*). There is also a possibility of Förster energy transfer (FET) between tetramethylrhodamine-4-dUTPs incorporated in different parts of the DNA. Fluorescence radiation emitted from incorporated tetramethylrhodamine-4-dUMP residues that is transferred by FET to G-binding tetramethylrhodamine-4-dUMPs will subsequently be quenched by electron transfer. Therefore, a linear relationship between the detected photocounts per DNA molecule in the FCS experiment and the number of fluorophores within the amplified DNA is only observed at low incorporation numbers when FET can be neglected.

Background Formation. The success of PCR is mainly determined by the proper choice of primers. However, experimental findings of real-time fluorescence quantification with ethidium bromide revealed that unspecific product formation becomes predominant at low numbers of initial template copies (*33*). In those experiments, aliquots of the PCR mixes were analyzed by gel electrophoresis. In the range of 10^8 down to 10^5 initial copies of the template, the only product found was that of the expected size. From 10^4 up to 10^2 template copies, a smaller nonspecific PCR product was detected. It was shown by Higuchi et al. (*33*) under nonoptimized conditions for low copy number amplification that the amount of nonspecific PCR product can be as high as the amount of the specific PCR product. Under the experimental PCR conditions discussed in the work presented, some amplified DNA molecules attain a higher diffusion time and thus are larger (called here the background) than the desired product. This is shown in Table 3 and Figure 4. There is more background formed in the PCR mixture the lower the initial template concentration, as can be seen in Figure 4. The size of the background varies between different preparations (different long diffusion times in Table 3 and Figure 4) and the amount of background formed is directly proportional to the amount of primer used in the PCR reaction. Moreover, the background was cleaved by the restriction enzymes used (data not shown), which were chosen to cleave the 217-bp product. All these observations

clearly indicate that this background is made of random sequences, including the primer sequences. It is well-known that a background may arise during the polymerization reaction due to nonspecific amplification. Competition with the targeted amplification can occur by primer oligomerization and mispriming. Under the experimental conditions used (low amount of primer), the formation of primer-dimers and/or concatemers (primer-ladders) is a low-probability event that could not be verified from the presented data. However, the lower the initial number of single-stranded templates, the greater the probability that mispriming occurs (*34*), as can be seen in the data in Table 3. Longer products can be created by primer extension of nonspecific or specific priming in early PCR cycles. They stay in PCR by forming networks among themselves, at sites of the original single-stranded template, for example. Using FCS cross-correlation analysis, we have established advanced PCR conditions for fluorescent labeling of DNA that suppress nonspecific amplification (*35*).

FCS-Based PCR Assays. The good model-to-reality correspondence found in our analysis (<2%) demonstrates that PCR products can be satisfactorily quantified by the approach presented herein. We avoid limitations of detection sensitivity in autocorrelation measurements when using primers labeled with one fluorophore only, as well as limitations arising from asymmetric PCR conditions at low initial template concentrations. It is therefore clear that the range of applicability of FCS analysis has been extended (*35*). The disadvantage with the method presented herein is that there is a need for removing the unincorporated tetramethylrhodamine-4-dUTP before measuring the FCS curve; otherwise the fluorescence signal from the free dye is too large and might overwhelm the measurement. Fortunately, this task can be performed quite easily and rapidly with MicroSpin columns (see Materials and Methods). With FCS cross-correlation this limitation is avoided (*35*) as well as in the amplified probe extension by FCS (*20*). The advantages of the FCS method presented herein are the extreme sensitivity and quickness of the measurement. Compared to the many steps required when performing gel electrophoresis, the measurement time of a few minutes is a large improvement in efficiency.

CONCLUSIONS

It is clear that the incorporation of tetramethylrhodamine-4-dUTP into the 217-bp M13mp18 DNA has been successful and that very low tetramethylrhodamine-4-dUTP concentrations are sufficient for detection. The detection sensitivity of FCS is extremely high, since when the samples were measured by FCS there was a need for dilutions of several orders of magnitude, while most of the samples presented herein were not detectable on agarose gels. The fact that a large "background" species is detected without using the template is also a reflection of the high sensitivity of FCS, since this is most likely not an artifact only occurring in our laboratory but rather a common PCR byproduct not often detected. The reproducibility between different preparations and experiments (~5%) is an indication of the reliability of the method. PCR has already proved to be a powerful tool for biochemists as well as molecular biologists. The combination of PCR with quantitative FCS methods is a potentially useful, quantitative biotechnique developed in our laboratory.

ACKNOWLEDGMENT

We thank Drs. Ülo Mets and Jerker Widengren for discussions and Lennart Wallerman for technical assistance. We also thank Professor Arne Holmgren for the gift of T7 exonuclease. M.K. thanks Professor T. Koyama (Hokkaido University) for continuous interest and support and Dr. H. Nakagomi (Karolinska Institute) for initial help with the PCR procedure.

REFERENCES

1. Magde, D., Elson, E. L., and Webb, W. W. (1972) *Phys. Rev. Lett. 29*, 705−711.
2. Ehrenberg, M., and Rigler, R. (1974) *Chem. Phys. 4*, 390−401.
3. Elson, E. L., and Magde, D. (1974) *Biopolymers 13*, 1−27.
4. Koppel, D. E. (1974) *Phys. Rev. A: Gen. Phys. A10*, 1938−1945.
5. Rigler, R., and Metz, Ü. (1992) *SPIE Laser Spectrosc. Biomol. 1921*, 239−248.
6. Rigler, R., Widengren, J., and Mets, Ü. (1992) in *Fluorescence Spectroscopy* (Wolfbeis, O. S., Ed.), pp 13-21, Springer, New York.
7. Rigler, R., Mets, Ü., Widengren, J., and Kask, P. (1993) *Eur. Biophys. J. 22*, 169−175.
8. Mets, Ü., and Rigler, R. (1994) *J. Fluoresc. 4*, 259−264.
9. Widengren, J., Mets, Ü., and Rigler, R. (1995) *J. Phys. Chem. 99*, 13368−13379.
10. Rigler, R. (1995) *J. Biotechnol. 41*, 177−186.
11. Eigen, M., and Rigler, R. (1994) *Proc. Natl. Acad. Sci. U.S.A. 91*, 5740−5747.
12. Maiti, S., Haupts, U., and Webb, W. (1997) *Proc. Natl. Acad. Sci. U.S.A. 94*, 11753−11757.
13. Földes-Papp, Z., Thyberg, P., Björling, S., Holmgren, A., and Rigler, R. (1997) *Nucleosides Nucleotides 16*, 781−787.
14. Marquardt, D. W. (1963) *J. Soc. Ind. Appl. Math. 11*, 431−441.
15. Provencher, S. W. (1982) *Comput. Phys. Commun. 27*, 213−227.
16. Provencher, S. W. (1982) *Comput. Phys. Commun. 27*, 229−242.
17. Rigler, R., Claesens, F., and Lomakka, G. (1984) in *Ultrafast Phenomena* (Auston, D. H., and Eisenthal, K. B., Eds.) Vol. 4, pp 472−476, Springer, Berlin.
18. Kovacic, R. T., and van Holde, K. E. (1977) *Biochemistry 16*, 1490−1498.
19. Kinjo, M., and Nishimura, G. (1997) *Bioimaging 5*, 134−138.
20. Walter, N. G., Schwille, P., and Eigen, M. (1996) *Proc. Natl. Acad. Sci. U.S.A. 93*, 12805−12810.
21. Kinjo, M. (1998) *Anal. Chim. Acta* (in press).
22. Yu, H., Chao, J., Patel, D., Mujumdar, R., and Mujumdar, S. (1994) *Nucleic Acids Res. 22*, 3226−3232.
23. Földes-Papp, Z., Angerer, B., Ankenbauer, W., Baumann, G., Birch-Hirschfeld, E., Björling, S., Conrad, S., Hinz, M., Rigler, R., Seliger, H., Thyberg, P., and Kleinschmidt, A. K. (1998) in *Fractals in Biology and Medicine* (Losa, G. A., Merlini, D., Nonnenmacher, T. F., and Weibel, E. R., Eds.), Vol. II, pp 238−254, Birkhäuser, Boston, MA.
24. Goodwin, P. M., Cai, H., Jett, J. H., Whang, S. L., Machura, N. P., Semin, D. J., Orden, A. V., and Keller, R. A. (1997) *Nucleosides Nucleotides 16*, 543−550.
25. Tanford, C. (1961) *Physical Chemistry of Macromolecules*, pp 327 and 342, Wiley, New York.
26. Broersma, S. (1960) *J. Chem. Phys. 32*, 1632−1635.
27. Bloomfield, V., Dalton, W. O., and Van Holde, K. E. (1967) *Biopolymers 5*, 135−148.

28. Bloomfield, V., Van Holde, K. E., and Dalton, W. O. (1967) *Biopolymers 5*, 149−159.
29. Sauer, M. Han, K.-T., Muller, R., Nord, S., Schultz, A., Seeger, S., Wolfrum, J., Arden-Jacobi, J., Deltau, G., Marx, N. J., Zander, C., and Drexhage, K. H. (1995) *J. Fluoresc. 5*, 247−261.
30. Widengren, J., Dapprich, J., and Rigler, R. (1997) *Chem. Phys. 216*, 417−426.
31. Edman, L., Mets, Ü., and Rigler, R. (1996) *Proc. Natl. Acad. Sci. 93*, 6710−6715.
32. Wennmalm, S., Edman, L., and Rigler, R. (1997) *Proc. Natl. Acad. Sci. U.S.A. 94*, 10641−10646.
33. Higuchi, R., Fockler, C., Dollinger, G., Watson, R. (1993) *Bio/Technology 11*, 1026−1030.
34. Chou, Q., Russell, M., Birch, D. E., Raymond, J., and Bloch, W. (1992) *Nucleic Acids Res. 20*, 1717−1723.
35. Rigler, R., Földes-Papp, Z., Meyer-Almes, F.-J., Sammet, C., Völcker, M., and Schnetz, A. (1998) *J. Biotechnol. 63*, 97−109.

BI980694C